Improvements on type-II Zeeman slowing of molecules through polarization selectivity

Qian Liang,[1] Wenhao Bu,[1] Yuhe Zhang,[1] Tao Chen,[1,*] and Bo Yan[1,2,3,†]

[1]*Interdisciplinary Center of Quantum Information, State Key Laboratory of Modern Optical Instrumentation, and Zhejiang Province Key Laboratory of Quantum Technology and Device of Physics Department, Zhejiang University, Hangzhou 310027, China*

[2]*Collaborative Innovation Centre of Advanced Microstructures, Nanjing University, Nanjing 210093, China*

[3]*Key Laboratory of Quantum Optics, Chinese Academy of Sciences, Shanghai 200800, China*

(Received 26 June 2019; revised manuscript received 16 September 2019; published 6 November 2019)

We propose a general Zeeman slower scheme applicable to the majority of the laser-coolable molecules. Different from previous schemes, we apply a careful modulation on the repump laser and guarantee the velocity selectivity through the polarization selection rules. Only atoms or molecules with the right velocity will be laser slowed. Such a scheme is more feasible for molecules with complex energy structures. We apply this scheme for molecules with a large Landé g factor of the excited states, i.e., $g_e > 0.1$, and polyatomic molecules with one-dimensional numerical simulations. The results show a better slowing efficiency with about 62% of the BaF molecules and 99% of the SrOH molecules being successfully slowed down to a velocity below 15 m/s without the consideration of transverse divergence.

DOI: 10.1103/PhysRevA.100.053402

I. INTRODUCTION

Ultracold molecules provide new research opportunities on precision measurement [1–3], ultracold chemistry [4], many-body physics [5–7], and quantum simulation [8–11]. Direct laser cooling on diatomic and polyatomic molecules with highly diagonal Franck-Condon factors [12,13] has achieved great success recently. The three-dimensional magnetooptical trap (MOT) has been demonstrated for SrF [12], CaF [14,15], and YO [13] molecules. Furthermore, the molasses of polar molecules has been realized [16], and some species have been loaded into the magnetic trap [17] and dipole trap [18]. Direct laser cooling of polar molecules has become a very hot topic recently.

However, one limitation is the poor molecule number captured in a MOT, usually about 10^3–10^5, much less than that for atoms. To push the direct cooling method further and achieve a higher phase-space density, a steady and efficient high-flux molecular source with slow-enough velocity distribution is highly required. Several techniques were demonstrated in previous experiments. The frequency-chirped slowing [19–21] is widely used and has a wonderful performance on producing a slowing molecular beam with a compressed velocity distribution in time. However, it works in a pulse mode and has a position-dependent distribution of the slowing particles [22]. While another white-light slowing [23,24] is continuous, but the velocity distribution cannot be compressed [23,25]. One way to get over those barriers is the Zeeman slower, which has good control on the final velocity and compresses the distribution simultaneously, making it promising to achieve a higher efficiency of molecular beam slowing and further a better implementation of MOT.

The traditional Zeeman slower working on atoms cannot be directly applied to molecules due to their complex internal structures. Recently, a type-II Zeeman slower was proposed [26] and experimentally demonstrated for ^{39}K atoms with the D1-line transition [27]. The magnetic field applied is in a rather strong regime up to ∼1000 G to enter the Pachen-Back regime, so the energy gap between every two hyperfine states in the same m_s manifold keeps almost the same under different magnetic field strength. In this way, the slowing scheme becomes greatly simplified and making the Zeeman slower feasible [see Fig. 1(a)]. The simulations in Ref. [26] showed that this scheme works well on the $|X^2\Sigma_{1/2}, N = 1, v = 0\rangle \rightarrow |A^2\Pi_{1/2}, J' = 1/2, v' = 0\rangle$ transition for the SrF molecule where the Landé g factor of the excited state g_Π is much smaller than that of the ground state g_Σ. However, it fails to effectively slow molecules with a large g factor for the upper state, for example, the BaF molecule with $g_\Pi \approx -0.202$. To go beyond this limitation, we need a more general Zeeman-slowing scheme.

Here we provide another view of the Zeeman slower by using the idea of the repump laser: instead of compensating the Doppler shift with the magnetic field on the cooling laser, we make such compensations on the repump laser. Molecules or atoms are hidden in the "dark state" until the repump laser is on resonance and make them back to the cycling transition. In this way, the velocity and the position are connected together and a Zeeman slower is realized. In the molecular case as shown in Fig. 1, the repump and cooling laser play a similar role and eventually this picture equal to the traditional Zeeman slower picture. However, in some cases if one state scatters much less photon to re-enter the cycling transition, this picture gives a better understanding. For a multilevel system such as the molecule, one "hidden" state is enough to make the Zeeman slower work. The less the state for molecules to hide, the easier the scheme to be realized.

With this picture in mind, we restructure the laser scheme as shown in Fig. 1(b). The key idea is that we use the

*phytch@zju.edu.cn
†yanbohang@zju.edu.cn

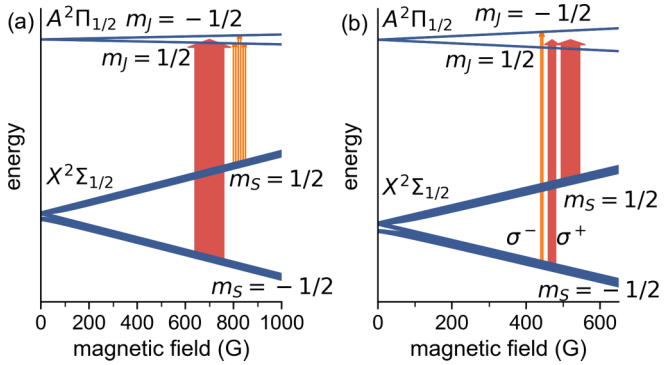

FIG. 1. Two different Zeeman slowing schemes for diatomic molecules: (a) laser scheme from Ref. [26] and (b) laser scheme in our enhanced type-II Zeeman slower. The hyperfine levels of the ground state $X^2\Sigma_{1/2}$ are separated as two manifolds with $m_S = \pm 1/2$, respectively. Each manifold has six sublevels. The excited state $A^2\Pi_{1/2}$ has four sublevels but the $m_I = \pm 1/2$ states are degenerate since the nuclear spin g factor is too small to affect the total Hamiltonian. For the SrF molecule in (a), the splitting of the $m_{J'} = \pm 1/2$ states is negligible while it is not the case for the BaF molecule in (b). The wide arrows (red) indicate the frequency-broadened repump laser in (a) and clean-up lasers in (b). The narrow arrows (orange) indicate the frequency-modulated slowing laser in (a) and repump laser in (b).

polarization of the repump laser to select only two sublevels to hide the molecule. Such a scheme is greatly simplified and shows a better slowing performance than that in Ref. [26] in the case with a large Landé g factor. The number of the slowed-down molecules (velocity smaller than 15 m/s) has been increased by ∼60% of the total in our enhanced Zeeman slower while no increase has occurred for the scheme in Fig. 1(a). In the following, we will discuss how this enhanced type-II Zeeman slower scheme works in Sec. II. Then, in Sec. III, we numerically simulate the one-dimensional deceleration process of the BaF molecule [28–30] with the rate equation approach, and compare the slowing result to that from the aforementioned type-II Zeeman slower scheme. Furthermore, we extend it to a laser-coolable polyatomic molecule, SrOH [31,32], to check its applicability and universality.

II. SCHEME DESCRIPTION AND METHOD

In a standard Zeeman slower [33], a position-dependent magnetic field compensates the change of the Doppler shift as the particles are continually decelerated. The slowing laser always keeps on- or near-resonance with the main cooling transition to efficiently slow the particles during the propagation. Both the type-I and type-II Zeeman slowers share such a basic compensation mechanism. But for type-II ones, the particles may accumulate into the unwanted dark states, making the slowing force vanish. Even if we destabilize the dark states by applying an angled magnetic field [34], the slowing laser cannot continually keep resonant due to the nonlinear energy shifts of the hyperfine sublevels, especially in the weak magnetic field regime. This prevents the conventional Zeeman slower from slowing the particles with type-II transitions. In Ref. [26], a large offset magnetic field $B_0 \sim 900$ G is introduced to simplify the choice of the cooling and repumping laser components; see Fig. 1(a). Under a large magnetic field, the electron spin decouples with the nuclear spin and rotational angular momentum. The sublevels in the ground state now are separated into two manifolds with $m_S = \pm 1/2$, respectively. The excited state, however, can be regarded as degenerate due to the small g factor compared to the ground state (for example, SrF [35] and YO [36] molecules). This makes the whole system reduce to a simple three-level system. Here, a slowing laser with six frequency sidebands couples the $m_S = +1/2$ states to the excited states according to the selection rules, while a frequency-broadened laser repumps the molecules that decay to the $m_S = -1/2$ manifold back to $m_S = +1/2$ for a wide velocity range. The repump laser must have a rather wide frequency range broadening up to about 1 GHz. To avoid the influence from the repump laser on the $m_S = -1/2$ manifold, the offset magnetic field should be large enough to split the $m_S = \pm 1/2$ manifolds away from each other. This type-II Zeeman slower has been proved to work as efficiently as the type-I Zeeman slower in a ^{39}K atom experiment [27].

It is obvious that the scheme only fits for molecules with a small upper g factor g_Π, otherwise the simplified three-level model collapses. When g_Π is no longer small enough, the splitting between the upper $m_{J'} = \pm 1/2$ states is considerably large even under a small magnetic field. Since the energy gap between the two upper $m_{J'}$ manifolds is large, the resonant frequencies of the six cooling transitions cannot change synchronously with the compensations from the magnetic field at the same time, leading to a less efficient slowing. Therefore, we propose an improved Zeeman slower scheme shown in Fig. 1(b). Similarly, we still apply an offset magnetic field to let the electron spin decoupled. Instead of applying a slowing laser with six frequencies to couple six hyperfine levels to the excited state, we use a broadened laser to couple four of the levels, and use two frequencies (we label them as the repump laser) for the last two levels. Velocity selectivity is retained by using a polarization of the two narrow lasers opposite to that of the broadened laser. In this way, it keeps molecules with the "wrong" velocity in the dark states while release them at the "right" velocity to get slowed at a specific position. When the Doppler shift mismatches the Zeeman shift, the molecule will be protected in the two *selected* levels and wait for the Zeeman shift to match again. In the end, the velocity distribution of the molecular beam can be compressed into a sharp and narrow distribution around a tunable final velocity.

To show the advantages of the enhanced slowing scheme in Fig. 1(b), we take the BaF molecule as an example. We choose the $|m_S = -1/2, m_N = +1, m_I = \pm 1/2\rangle$ states as the *selected* states and the laser polarization to be σ^- to make them only coupled to the excited $|m_{J'} = -1/2, m_{I'} = \pm 1/2\rangle$ states, respectively. The polarization of the laser that drives all the other states in the $m_S = -1/2$ manifold is chosen to be σ^+, such that the selected transitions will not be disturbed by it. Another laser that drives the ground $m_S = +1/2$ manifold is also required, and similarly we apply an offset magnetic field to enter the Pachen-Bach regime. The repump laser and the clean-up laser works on the $m_S = -1/2$ manifold interact with the moving molecule independently. So we only need to prevent the clean-up laser that works on the $m_S = +1/2$

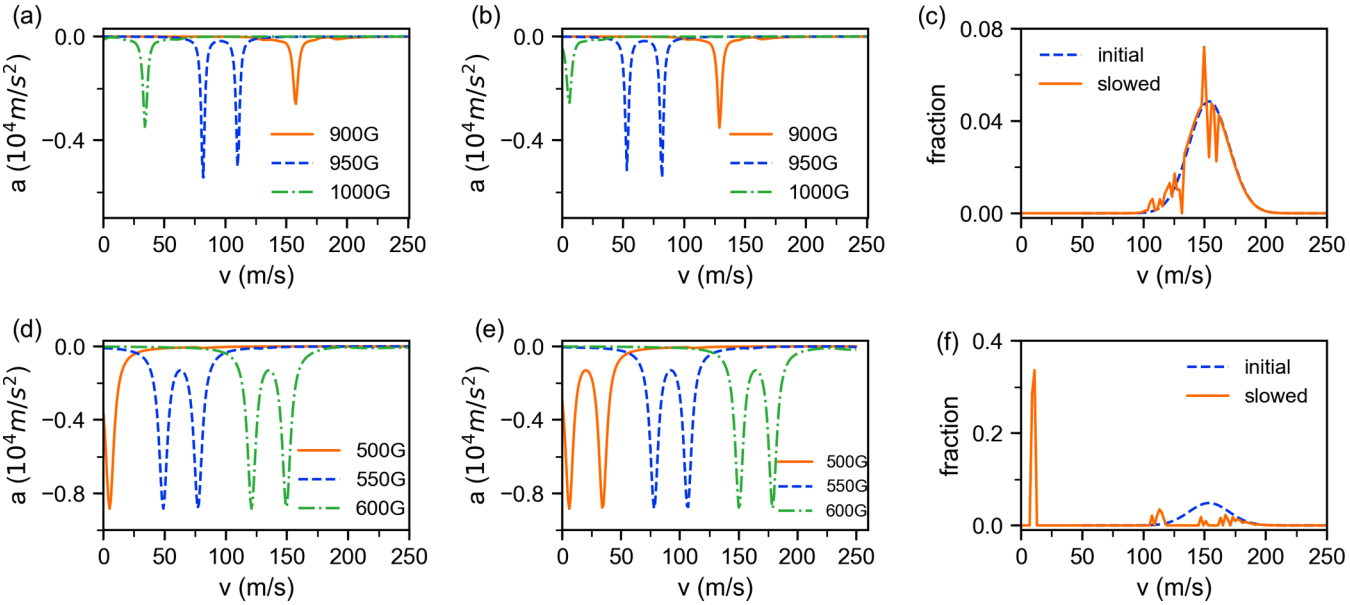

FIG. 2. (a) The velocity-dependent deceleration rate of the molecules in $m_I = -1/2$ manifold under different magnetic field for the type-II Zeeman slower scheme in Fig. 1(a). (b) The velocity-dependent deceleration rate of the molecules in $m_I = +1/2$ manifold under different magnetic field for the type-II Zeeman slower scheme in Fig. 1(a). (c) The initial velocity distribution (blue dotted line) and the final velocity distribution after the deceleration of the type-II Zeeman slower (orange solid line). (d) The velocity-dependent deceleration rate of the molecules in $m_I = -1/2$ manifold under different magnetic field with our enhanced type-II Zeeman slower scheme shown in Fig. 1(b). (e) The velocity-dependent deceleration rate of the molecules in $m_I = +1/2$ manifold under different magnetic field with our enhanced type-II Zeeman slower scheme shown in Fig. 1(b). (f) The initial velocity distribution (blue dotted line) and the final velocity distribution after the deceleration of the enhanced Zeeman slower (orange solid line).

manifold from disturbing the repump laser. In a magnetic field of 500 G, the center of the $m_S = +1/2$ ground states have an energy gap of 1.43 GHz with the *selected* states, which is large enough to avoid the possible influence. In our scheme, the Landé g factor of the excited state is no longer a restriction since the repump laser couples the *selected* states to the same upper $m_{J'}$ manifold.

We use the multilevel rate equation approach to calculate the slowing force for different moving velocities, and then simulate the slowing process of a molecular beam with an initial velocity distribution [37]

$$f(v) = Av^2 e^{-\beta(v-v_0)^2}, \tag{1}$$

where A is the normalization parameter, β is related to the temperature and the molecular mass, and v_0 is the center velocity. The multilevel rate equations can be derived from the optical Bloch equation as [38]

$$\frac{dN_l}{dt} = \sum_{u,p} R_{l,u,p}(N_u - N_l) + \Gamma \sum_u r_{l,u} N_u,$$
$$\frac{dN_u}{dt} = \sum_{l,p} R_{l,u,p}(N_l - N_u) - \Gamma N_u, \tag{2}$$

where N_u and N_l are the populations of the excited state $|u\rangle$ and ground state $|l\rangle$, respectively, $r_{l,u}$ is the branching ratio of the decay from the upper $|u\rangle$ state to the ground $|l\rangle$ state, and Γ is the decay rate of the excited state. The excitation rate from $|l\rangle$ to $|u\rangle$ by the pth beam is given by

$$R_{l,u,p} = \frac{\Gamma}{2} \frac{r_{l,u} s_p}{1 + 4\Delta_{l,u}^2/\Gamma^2}, \tag{3}$$

with s_p is the saturation parameter. $\Delta_{l,u}$ is the detuning between $|u\rangle$ and $|l\rangle$, including both the Zeeman shift and the Doppler shift. The radiative force can be obtained from the number of the scattered photons, i.e.,

$$\vec{F} = \sum_{l,u,p} \hbar \vec{k}_p R_{l,u,p}(N_u - N_l), \tag{4}$$

with $\vec{k}_p$ the wave vector of the pth beam.

We assume that the molecules are in the 12 sublevels of the ground state evenly at the initial stage. Then we let the states evolve with the rate equation. The force induced by the laser is calculated by Eq. (4) when the internal state becomes stable.

III. SIMULATION AND COMPARISON

A. BaF molecule

The BaF molecule is a candidate for direct laser cooling and the molecular structures and branching ratios have already been investigated in detail [28]. In Fig. 2, we show the different slowing results for the BaF molecule with the two schemes mentioned in Fig. 1. In both schemes, we assume that a set of molecules enter the Zeeman slower with an initial velocity distribution as Eq. (1); see Fig. 2(c). At the end of the Zeeman slower we count the molecular number in each velocity and give a final statistic distribution. For the one shown in Fig. 1(a), we set the position-dependent magnetic field with the formula [27]

$$B = B_0 + \alpha L(1 - \sqrt{1 - z/L}), \tag{5}$$

in which B_0 is the offset magnetic field, α is the magnetic field gradient, z is the position of the molecule and L is the total length of the slower. Here we set $L = 1.8$ m, $B_0 = 900$ G, $\alpha = 58.3$ G/m, leading to a maximum magnetic field of $B_{\max} = 1005$ G. The slowing laser is sideband-modulated carefully to be on-resonance with each slowing transition at $B = 950$ G and the velocity $v = 80$ m/s. The saturation parameter for each slowing beam is $s = 2$, while the repump laser takes $s = 72$ with a frequency bandwidth of 1.2 GHz.

For our enhanced type-II Zeeman slower scheme in Fig. 1(b), the magnetic field has a monotonically decreasing form

$$B = B_0 + \alpha L\sqrt{1 - z/L}. \tag{6}$$

The difference between the two magnetic field, i.e., Eqs. (5) and (6), comes from the choices of different m_S quantum numbers of the ground states that do the compensation. The parameters we use here are $B_0 = 500$ G, $\alpha = 61$ G/m, and $L = 1.8$ m. The saturation parameters of two frequency components in the repump laser are $s = 2$, and they are set to be on-resonance, respectively, with the transitions of $|m_S = -1/2, m_N = +1, m_I = \pm 1/2\rangle \rightarrow |m_{J'} = -1/2, m_{I'} = \pm 1/2\rangle$ at a specific position and velocity. The bandwidth of the broadened clean-up laser that pumps the rest states in $m_S = -1/2$ manifold is broadened to be 400 MHz, and its saturation parameter $s = 8$. For the laser that pumps the $m_S = +1/2$ manifold, the bandwidth is 800 MHz and the saturation parameter $s = 72$. The initial velocity distribution centering at 150 m/s (from 50 to 250 m/s) is estimated by Eq. (1) to be a good approximation to the experimental measurement.

Due to the selection rule that $\Delta m_I = 0$, the molecule will stay in each m_I manifold during the slowing process. The slowing forces for molecules initially in $m_I = +1/2$ and $m_I = -1/2$ show different profiles due to the energy shift of the two manifolds, as shown in Figs. 2(a) and 2(b), respectively, for the scheme in Fig. 1(a) while in Figs. 2(d) and 2(f), respectively, for our enhanced one. For both cases with $m_I = +1/2$ and $m_I = -1/2$, the type-II Zeeman slower scheme in Ref. [26] cannot provide a large and stable slowing force for the BaF molecule as the magnetic field changes. When the magnetic field goes away from the center point $B = 950$ G, the absolute value of the deceleration rate rapidly decreases. The reason lies in that the states in $m_S = +1/2$ manifold are coupled to different excited states, i.e., $|m_S = +1/2, m_N = 0, m_I = \pm 1/2\rangle \rightarrow |m_{J'} = -1/2, m_{I'} = \pm 1/2\rangle$ and $|m_S = +1/2, m_N = \pm 1, m_I = \pm 1/2\rangle \rightarrow |m_{J'} = +1/2, m_{I'} = \pm 1/2\rangle$. The energy splitting of the $m_{J'} = \pm 1/2$ states show different behaviors when the magnetic field increases, resulting in that the slowing laser cannot be resonant with the molecules all the time. In contrast, the slowing force of our enhanced Zeeman slower is robust to the change of the magnetic field. By adjusting the magnetic field, one can always obtain a stable deceleration maximum to -8000 m/s^2. The two-frequencies modulation of the repump laser provides two chances for a molecule at different velocities to get on-resonance, which leads to the two nearly equal acceleration peaks in Figs. 2(d) and 2(f). Apparently, the slowing force profiles of molecules with different m_I have a velocity shift with each other at the same magnetic field.

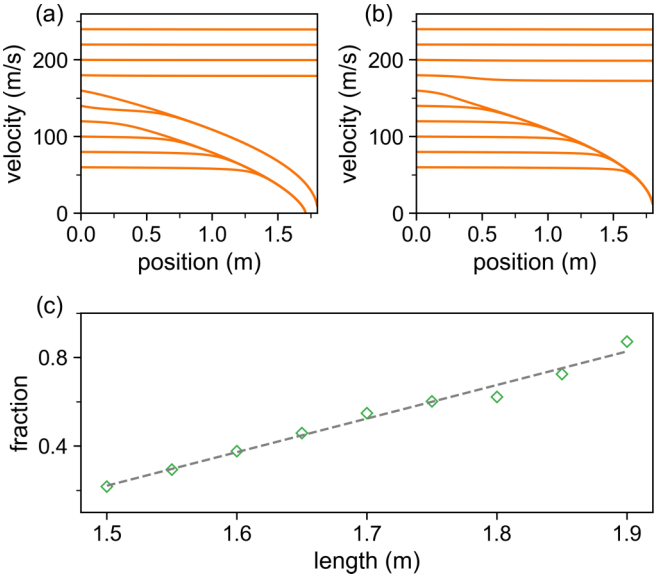

FIG. 3. (a) The position-dependent evolutions of molecules in $m_I = -1/2$ with different initial velocities from 50 to 250 m/s. (b) The position-dependent evolutions of molecules in $m_I = +1/2$. (c) The dependence of the final compressed molecular fraction below 15 m/s on the length of the Zeeman slower.

A comparison of the slowing effect from the two different schemes is shown in Figs. 2(c) and 2(f). For the old one, with the parameters described above, the final velocity distribution slightly changes, and only a small fraction of BaF molecules get decelerated; see Fig. 2(c). However, with our improved scheme, the slowing effect gets greatly enhanced. As shown in Fig. 2(f), about 62% of the BaF molecules are slowed to a velocity below 15 m/s. Note that here we only consider one-dimensional slowing. In a real slowing experiment, the transverse divergence of the molecular beam should be taken into consideration [39], which will greatly weaken the low-velocity fraction of the molecules. Nevertheless, our simulations here show an effective slowing to make the beam converge to a narrow distribution around a low velocity. Such an enhancement makes it possible to load a MOT with a considerable molecular number.

Figures 3(a) and 3(b) show the trajectory of the moving molecules with different initial velocities when they pass through the enhanced type-II Zeeman slower. Molecules with different m_I quantum numbers have different moving behaviours. Figure 2 tells us that molecules in $m_I = -1/2$ would get slowed earlier than the ones in $m_I = +1/2$ with a same velocity, especially in the small velocity region. In Fig. 3(a), molecules with a velocity less than 120 m/s get decelerated down to zero velocity before reaching the end of the Zeeman slower and then experience an acceleration in the opposite direction. In our simulation, we take this part as a loss. Molecules with a rather large velocity, i.e., $v > 170$ m/s, always stay in a far-off detuning condition and no deceleration happens at all as the magnetic field changes. In Fig. 3(b), most molecules are well decelerated. They are protected in the *selected* states at the early stage of the slowing, and then get

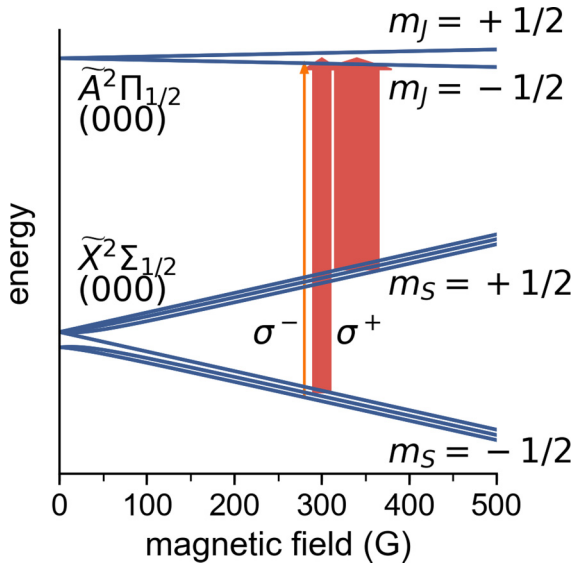

FIG. 4. The structure of the $\widetilde{X}^2\Sigma_{1/2}(000)$ and $\widetilde{A}^2\Pi_{1/2}(000)$ of SrOH molecule (necessary data from Ref. [40]) and the laser scheme applied. The vibrational quantum numbers $(v_1v_2v_3)$ correspond to the Sr ↔ OH stretching (v_1), Sr-O-H bending(v_2) and SrO ↔ H stretching (v_3) vibrational modes. There are 12 sublevels in the $\widetilde{X}^2\Sigma_{1/2}(000)$ state, but the $m_I = \pm 1/2$ states are degenerate. A repump laser (the narrow orange arrow) is applied to couple the $|m_s = -1/2, m_N = 1, m_I = \pm 1/2\rangle$ states with the corresponding excited states. Two clean-up lasers pumps the rest of the states (the wide red arrows).

slowed at a specific position where the Doppler shift and the Zeeman shift match each other. The velocity range in which the molecules can be effectively slowed is determined by both the detuning of the repump laser and the distribution of the magnetic field (i.e., the gradient).

The slowing efficiency also depends on the length of the slower. Apparently, longer length leads to molecules with higher velocity being slowed down. As shown in Fig. 3(c), the slowed fraction below 15 m/s increases as the length L increases. Here the offset magnetic field $B_0 = 500$ G and the gradient $\alpha = 61$ G/m are fixed for various lengths in our simulation. Apparently, longer length leads to molecules with higher velocity being slowed down. With careful adjustment of the magnetic field and the detuing of the laser, an efficiency nearly to 100% is attainable. Another issue is that the Zeeman slower for the BaF molecule should be long enough to obtain better efficiency as the radiative force is small compared to some other laser-coolable molecules. In an actual experiment, a suitable compromise of the slower length and the transverse divergence should be taken into account.

B. SrOH molecule

To demonstrate the universality of our enhanced type-II Zeeman slower scheme, we check its applicability on a polyatomic molecule SrOH. The structure of the SrOH is much more complicated than the diatomic molecule for it contains three vibrational modes, including degenerated bending vibrations [41]. Optical cycling on a quasiclosed transition and further sub-Doppler cooling have been realized [32,42]. Here we work on the main cooling transition,

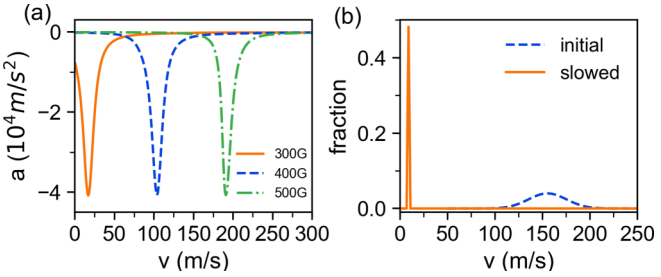

FIG. 5. (a) The deceleration rate versus the velocity under different magnetic field. (b) The initial velocity distribution (blue dotted line) and the final slowed velocity distribution (orange solid line).

i.e., $\widetilde{X}^2\Sigma_{1/2} \rightarrow \widetilde{A}^2\Pi_{1/2}$ transition. The splitting between the two $|m_S, m_N, m_I = \pm 1/2\rangle$ states is about ∼1 MHz, and they are nearly degenerate, as shown in Fig. 4. Here only a single-frequency repump laser is enough, and no sideband modulations are required. In our simulation, the repump laser has a saturation parameter of $s = 2$, coupling the ground states $|m_S = -1/2, m_N = 1, m_I = \pm 1/2\rangle$ to $|m_{J'} = -1/2, m_{I'} = \pm 1/2\rangle$. The clean-up laser coupling the rest of the states in the $m_S = -1/2$ manifold has a saturation parameter of $s = 8$ and a broadened frequency width of 180 MHz, while the other with $s = 72$ and a broadened bandwidth of 700 MHz.

Figure 5(a) shows the velocity-dependent deceleration rate for the SrOH molecule. The absolute value of deceleration rate can be up to -4×10^4 m/s^2, which is considerably large enough to slow the molecules. The slowing forces are stable and share a similar shape under different magnetic field strength. This indicates that our scheme can be directly extended to the SrOH molecule. Note that because the slowing laser has only one frequency, the deceleration profile under a specific magnetic field only has one dip in Fig. 5(a), different from that for the BaF molecule in Fig. 2.

The distribution of the magnetic field of the slower still follows the formula of Eq. (6), ranging from 540 to 292 G. The length of the slower is $L = 1$ m. Figure 5(b) shows the slowing effect. About 99% of the molecules get slowed below 11 m/s without consideration on the transverse divergence. The results discussed above show that the enhanced type-II scheme is capable of slowing polyatomic molecules that have a quasiclosed cycling transition.

IV. CONCLUSION

In summary, we propose a general type-II Zeeman slower that can decelerate most species of molecules that can be laser cooled. Such a scheme makes it possible to slow molecules that have a relatively large g factor of the excited state. Different from the traditional Zeeman slower used in atoms, an offset magnetic field is indispensable, and some frequency-broadened lasers are required to avoid molecules accumulating in dark states. In our scheme, the requirements on the magnetic field and the frequency-broadened clean-up lasers are accessible in the current experiments. Here we only consider the main vibrational transition, while in the real experiment, vibrational repumping is necessarily required. To compensate for the Doppler shift of the molecules, the

frequency of the vibrational repump laser will also be broadened. The slowing effect can be retained with an appropriate laser scheme. Our simulations show that our scheme can efficiently slow molecules to a small velocity under 15 m/s and significantly compress the distribution of the velocity. We expect this enhanced type-II Zeeman slower serves as a molecular source to increase the MOT loading rate and molecular number in future laser-cooling experiments.

ACKNOWLEDGMENTS

We acknowledge the support from the National Natural Science Foundation of China under Grant No. 91636104, the National Key Research and Development Program of China under Grant No.2018YFA0307200. The Natural Science Foundation of Zhejiang province under Grant No. LZ18A040001, and the Fundamental Research Funds for the Central Universities are also acknowledged.

[1] C. Chin, V. V. Flambaum, and M. G. Kozlov, New J. Phys. **11**, 055048 (2009).

[2] D. DeMille, S. B. Cahn, D. Murphree, D. A. Rahmlow, and M. G. Kozlov, Phys. Rev. Lett. **100**, 023003 (2008).

[3] M. S. Safronova, D. Budker, D. DeMille, D. F. J. Kimball, A. Derevianko, and C. W. Clark, Rev. Mod. Phys. **90**, 025008 (2018).

[4] S. Ospelkaus, K.-K. Ni, D. Wang, M. H. G. de Miranda, B. Neyenhuis, G. Quéméner, P. S. Julienne, J. L. Bohn, D. S. Jin, and J. Ye, Science **327**, 853 (2010).

[5] D.-W. Wang, M. D. Lukin, and E. Demler, Phys. Rev. Lett. **97**, 180413 (2006).

[6] I. Bloch, J. Dalibard, and W. Zwerger, Rev. Mod. Phys. **80**, 885 (2008).

[7] B. Yan, S. A. Moses, B. Gadway, J. P. Covey, K. R. A. Hazzard, A. M. Rey, D. S. Jin, and J. Ye, Nature **501**, 521 (2013).

[8] D. DeMille, Phys. Rev. Lett. **88**, 067901 (2002).

[9] A. André, D. DeMille, J. M. Doyle, M. D. Lukin, S. E. Maxwell, P. Rabl, R. J. Schoelkopf, and P. Zoller, Nat. Phys. **2**, 636 (2006).

[10] A. Micheli, G. K. Brennen, and P. Zoller, Nat. Phys. **2**, 341 (2006).

[11] P. Rabl, D. DeMille, J. M. Doyle, M. D. Lukin, R. J. Schoelkopf, and P. Zoller, Phys. Rev. Lett. **97**, 033003 (2006).

[12] J. F. Barry, D. J. McCarron, E. B. Norrgard, M. H. Steinecker, and D. DeMille, Nature **512**, 286 (2014).

[13] A. L. Collopy, S. Ding, Y. Wu, I. A. Finneran, L. Anderegg, B. L. Augenbraun, J. M. Doyle, and J. Ye, Phys. Rev. Lett. **121**, 213201 (2018).

[14] L. Anderegg, B. L. Augenbraun, E. Chae, B. Hemmerling, N. R. Hutzler, A. Ravi, A. Collopy, J. Ye, W. Ketterle, and J. M. Doyle, Phys. Rev. Lett. **119**, 103201 (2017).

[15] K. N. Jarvis, J. A. Devlin, T. E. Wall, B. E. Sauer, and M. R. Tarbutt, Phys. Rev. Lett. **120**, 083201 (2018).

[16] S. Truppe, H. J. Williams, M. Hambach, L. Caldwell, N. J. Fitch, E. A. Hinds, B. E. Sauer, and M. R. Tarbutt, Nat. Phys. **13**, 1173 (2017).

[17] H. J. Williams, L. Caldwell, N. J. Fitch, S. Truppe, J. Rodewald, E. A. Hinds, B. E. Sauer, and M. R. Tarbutt, Phys. Rev. Lett. **120**, 163201 (2018).

[18] L. Anderegg, B. L. Augenbraun, Y. Bao, S. Burchesky, L. W. Cheuk, W. Ketterle, and J. M. Doyle, Nat. Phys. **14**, 890 (2018).

[19] S. Truppe, H. J. Williams, N. J. Fitch, M. Hambach, T. E. Wall, E. A. Hinds, B. E. Sauer, and M. R. Tarbutt, New J. Phys. **19**, 022001 (2017).

[20] M. Yeo, M. T. Hummon, A. L. Collopy, B. Yan, B. Hemmerling, E. Chae, J. M. Doyle, and J. Ye, Phys. Rev. Lett. **114**, 223003 (2015).

[21] V. Zhelyazkova, A. Cournol, T. E. Wall, A. Matsushima, J. J. Hudson, E. A. Hinds, M. R. Tarbutt, and B. E. Sauer, Phys. Rev. A **89**, 053416 (2014).

[22] W. Ertmer, R. Blatt, J. L. Hall, and M. Zhu, Phys. Rev. Lett. **54**, 996 (1985).

[23] J. F. Barry, E. S. Shuman, E. B. Norrgard, and D. DeMille, Phys. Rev. Lett. **108**, 103002 (2012).

[24] B. Hemmerling, E. Chae, A. Ravi, L. Anderegg, G. K. Drayna, N. R. Hutzler, A. L. Collopy, J. Ye, W. Ketterle, and J. M. Doyle, J. Phys. B **49**, 174001 (2016).

[25] M. Zhu, C. W. Oates, and J. L. Hall, Phys. Rev. Lett. **67**, 46 (1991).

[26] M. Petzold, P. Kaebert, P. Gersema, M. Siercke, and S. Ospelkaus, New J. Phys. **20**, 042001 (2018).

[27] M. Petzold, P. Kaebert, P. Gersema, T. Poll, N. Reinhardt, M. Siercke, and S. Ospelkaus, Phys. Rev. A **98**, 063408 (2018).

[28] T. Chen, W. Bu, and B. Yan, Phys. Rev. A **94**, 063415 (2016).

[29] W. Bu, T. Chen, G. Lv, and B. Yan, Phys. Rev. A **95**, 032701 (2017).

[30] T. Chen, W. Bu, and B. Yan, Phys. Rev. A **96**, 053401 (2017).

[31] I. Kozyryev, L. Baum, K. Matsuda, P. Olson, B. Hemmerling, and J. M. Doyle, New J. Phys. **17**, 045003 (2015).

[32] I. Kozyryev, L. Baum, K. Matsuda, B. Hemmerling, and J. M. Doyle, J. Phys. B **49**, 134002 (2016).

[33] W. D. Phillips and H. Metcalf, Phys. Rev. Lett. **48**, 596 (1982).

[34] D. J. Berkeland and M. G. Boshier, Phys. Rev. A **65**, 033413 (2002).

[35] E. S. Shuman, J. F. Barry, and D. DeMille, Nature **467**, 820 (2010).

[36] M. T. Hummon, M. Yeo, B. K. Stuhl, A. L. Collopy, Y. Xia, and J. Ye, Phys. Rev. Lett. **110**, 143001 (2013).

[37] S. Truppe, M. Hambach, S. M. Skoff, N. E. Bulleid, J. S. Bumby, R. J. Hendricks, E. A. Hinds, B. E. Sauer, and M. R. Tarbutt, J. Mod. Opt. **65**, 648 (2018).

[38] M. O. Scully and M. S. Zubairy, *Quantum Optics* (Cambridge University Press, Cambridge, England, 1997).

[39] J. F. Barry, E. S. Shuman, and D. DeMille, Phys. Chem. Chem. Phys. **13**, 18936 (2011).

[40] D. A. Fletcher, K. Y. Jung, C. T. Scurlock, and T. C. Steimle, J. Chem. Phys. **98**, 1837 (1993).

[41] P. I. Presunka and J. A. Coxon, Chem. Phys. **190**, 97 (1995).

[42] I. Kozyryev, L. Baum, K. Matsuda, B. L. Augenbraun, L. Anderegg, A. P. Sedlack, and J. M. Doyle, Phys. Rev. Lett. **118**, 173201 (2017).